Original Article: Open Access

VIBGYOR ePress

International Journal of
Nanoparticles and Nanotechnology

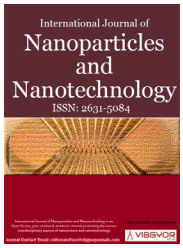

ISSN: 2631-5084

Preparation and Magnetic Properties of Fe Doped Zno Thin Films with Dilute Magnetic Semiconductors

***Yidong Zhang*, Jing Liu and Yuanhao Gao**

Key Laboratory for Micro-Nano Energy Storage and Conversion Materials of Henan Province, Institute of Surface Micro and Nano Materials, Xuchang University, Xuchang, China

Abstract

Fe doped ZnO solid solution and its semiconductor thin films were prepared by sol-gel method. After aging and quenching, the films were characterized by X-ray diffraction (XRD) and atomic force microscopy (AFM). The elemental proportion was obtained by energy dispersive spectrometer (EDS) and the magnetic properties were measured by magnetic force microscope (MFM). The results show that iron doping can inhibit the growth of zinc oxide particles, and then increase the roughness of thin films. The results of MFM show that Fe doping can make non-magnetic ZnO semiconductors become dilute magnetic semiconductors. With the increasing amount of Fe doping, the distribution of magnetic domains and magnetic moments becomes more obvious.

Keywords

Sol-gel, Fe-doped ZnO thin films, Magnetic force microscopy (MFM), Ferromagnetism

Introduction

With the development of spintronics, diluted magnetic semiconductors (DMSs), as the main research materials, have been extensively explored. DMSs have excellent magnetic, magneto-optic and magnetoelectronic properties, and have important applications in high-density nonvolatile memory, magnetic inductors, optical isolators, semiconductor integrated circuits, semiconductor lasers and spin quantum computers [1]. Zinc oxide is a multifunctional broadband semiconductor. Its band gap at room temperature is about 3.37 eV [2]. Because of its high melting point (1975 °C) and high chemical and thermal stability, zinc oxide can be doped as a matrix to obtain thin magnetic semiconductor films, while zinc oxide single crystal films can be obtained at temperatures below 500 °C [3]. Therefore, the defects produced by high temperature preparation can be greatly reduced by high temperature quenching [4] As a wide band gap semiconductor, ZnO has shown more and more important research value and potential application value. There are many methods for preparing ZnO, such as precipitation [5], hydrothermal [6] and electrospinning [7]. Especially, sol-gel is a very promising method with the characteristics of high purity, good uniformity, fine particle size, low synthetic temperature and simple process equipment [8].

***Corresponding author:** *Yidong Zhang, Key Laboratory for Micro-Nano Energy Storage and Conversion Materials of Henan Province, Institute of Surface Micro and Nano Materials, Xuchang University, Xuchang, 461000, P.R. China, Tel: +86-374-2968783*

Accepted: June 06, 2019; **Published:** June 08, 2019

ISSN 2631-5084

9 772631 508002

Citation: Zhang Y, Liu J, Gao Y (2019) Preparation and Magnetic Properties of Fe Doped Zno Thin Films with Dilute Magnetic Semiconductors. Int J Nanoparticles Nanotech 5:028

The strong exchange between carriers and local magnetic moments changes the band structure and the behavior of carriers, which makes DMSs present many new physical phenomena [9]. The theory shows that the wide bandgap semiconductor ZnO may have a higher Curie temperature [10], which makes the ZnO-based DMS materials become one of the research hotspots. Shinde, et al. studied the electronic structure and magnetic properties of Ni-doped ZnO nanopowders. It was found that the different doping positions resulted in three different coupling states of ferromagnetism, antiferromagnetism and paramagnetism [11]. Presently, there are few theoretical studies on Fe-doped ZnO films [12].

In this study, EDS and XRD were used to investigate the crystal structure and the proportion of atoms. MFM was used to study the surface roughness, magnetic domains and magnetic moments of Fe-doped ZnO thin film.

Experimental Procedure

All the reagents used in the experiments were in analytic grade (purchased from Shanghai Sinopharm Chemical Reagent Co., Ltd) and used without further purification.

Preparation of Fe-doped ZnO thin films

ZnO sols were fabricated by sol-gel method using zinc acetate, anhydrous ethanol, and diethanolamine (DMA) as the solute, solvent, and sol stabilizer, respectively. In a typical procedure, zinc acetate was first dissolved in ethanol at 50 °C, then DMA and a certain amount of iron acetate was slowly added into the solution under fierce stirring for an hour to form transparent Fe-doped ZnO mixed sols. The amount of iron acetate was controlled according to the molar ratio between ZnO and Fe. In the sol, the molar ratio of DMA to zinc acetate was kept at 1.0, and the Zn concentration was 0.5 M. Then Fe-doped ZnO thin films were prepared by a spin coating method on glass substrates for 30 sec with a spinning speed of 2000 rpm. The glass substrates were ultrasonically cleaned by ethanol, acetone, and distilled water for 30 min, respectively. After the spin coating, the resulting Fe-doped ZnO (x = 0, 1, 5, and 10 mol%) thin films were annealed at 500 °C in air for 1 h, which are marked with a, b, c and d, respectively.

The crystal structure of Fe-doped ZnO thin films were determined by XRD (Bruker D8 advance; Germany) with Cu Ka radiation (1.54 Å) operating at 40 kV. The surface morphology and magnetic domains of the thin films were observed by MFM, (Bruker Dimension ICON, Nanoscope V) at a scan rate of 1.0 Hz with commercial CoCr coated silicon

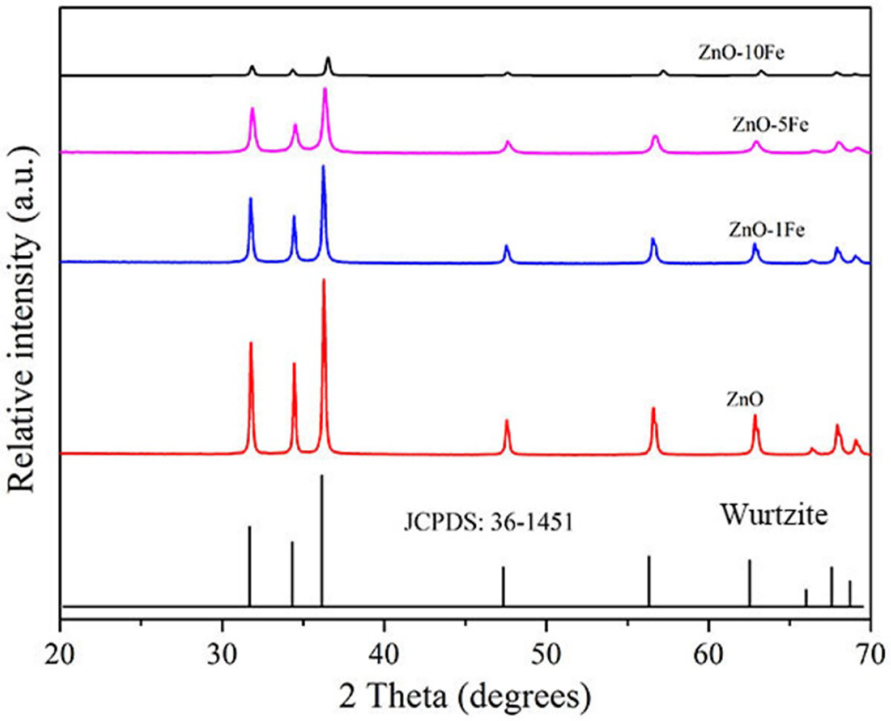

Figure 1: XRD of Fe-doped ZnO.

probe under ambient conditions (25 °C). The tip radius, spring constant, and resonance frequency of the probe are less than 10 nm, 2.8 N/m, and 75 kHz, respectively.

Result and Discussion

The XRD patterns of ZnO thin films with different Fe content annealed at 500 °C are shown in Figure 1. The diffraction peaks of samples, which corresponded to (100), (002) and (101) of standard ZnO powder, indicating that the samples were polycrystalline hexagonal wurtzite structure (Zincite, JCPDS 36-1451). It can be seen that the half-peak width increases with the increase of Fe doping. According to Scheller's formula [13],

$$D = \frac{k\lambda}{\beta cos\theta} \quad (1)$$

Where k = 0.9 is the shape factor, λ is the x-ray wavelength of Cu Kα radiation (1.54 Å), θ is the Bragg diffraction angle, and β is the full width at half maximum of the respective diffraction peak. The larger the half-peak width, the smaller the grain size, i.e. more small grains are produced, indicating that a certain amount of Fe can inhibit the grain growth of zinc oxide.

EDS spectrum of as prepared Fe-doped ZnO thin films is shown in Figure 2, which reveals the atomic ratio of Zn and O in the products that is less than the stoichiometric ratio (1.2: 1), leading to the formation of oxygen vacancies. A relatively weak carbon and oxygen peaks in the spectrum probably originates from unavoidable surface contaminative carbon and surface-adsorption of oxygen on the surface of sample from exposure to air during sample preparing. After doping Fe atoms in ZnO, the atomic ratio of Zn to O is decreased to 1.18:1,

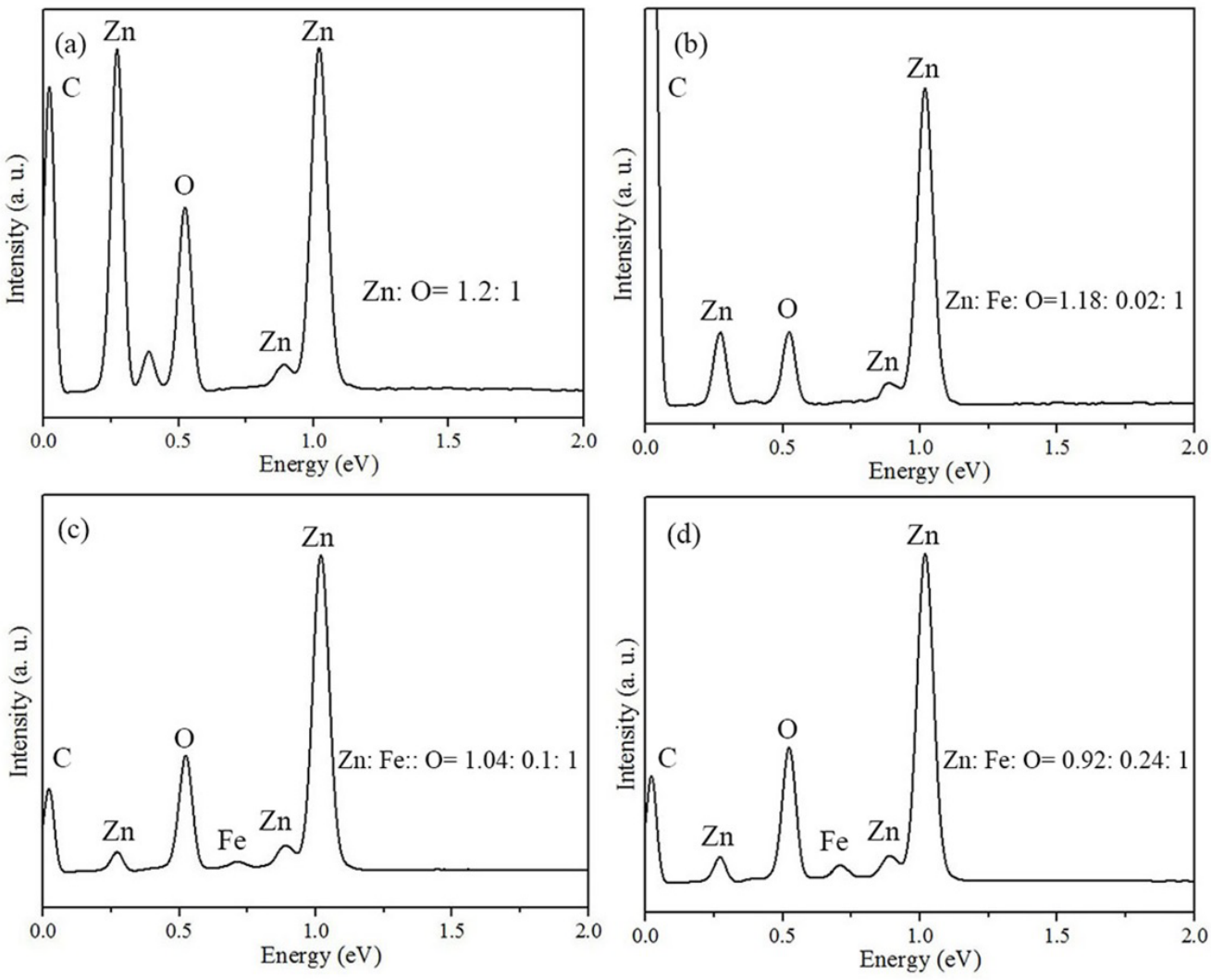

Figure 2: EDS of Fe-doped ZnO with different Fe contents: a) 0; b) 1%; c) 5%; d) 10%.

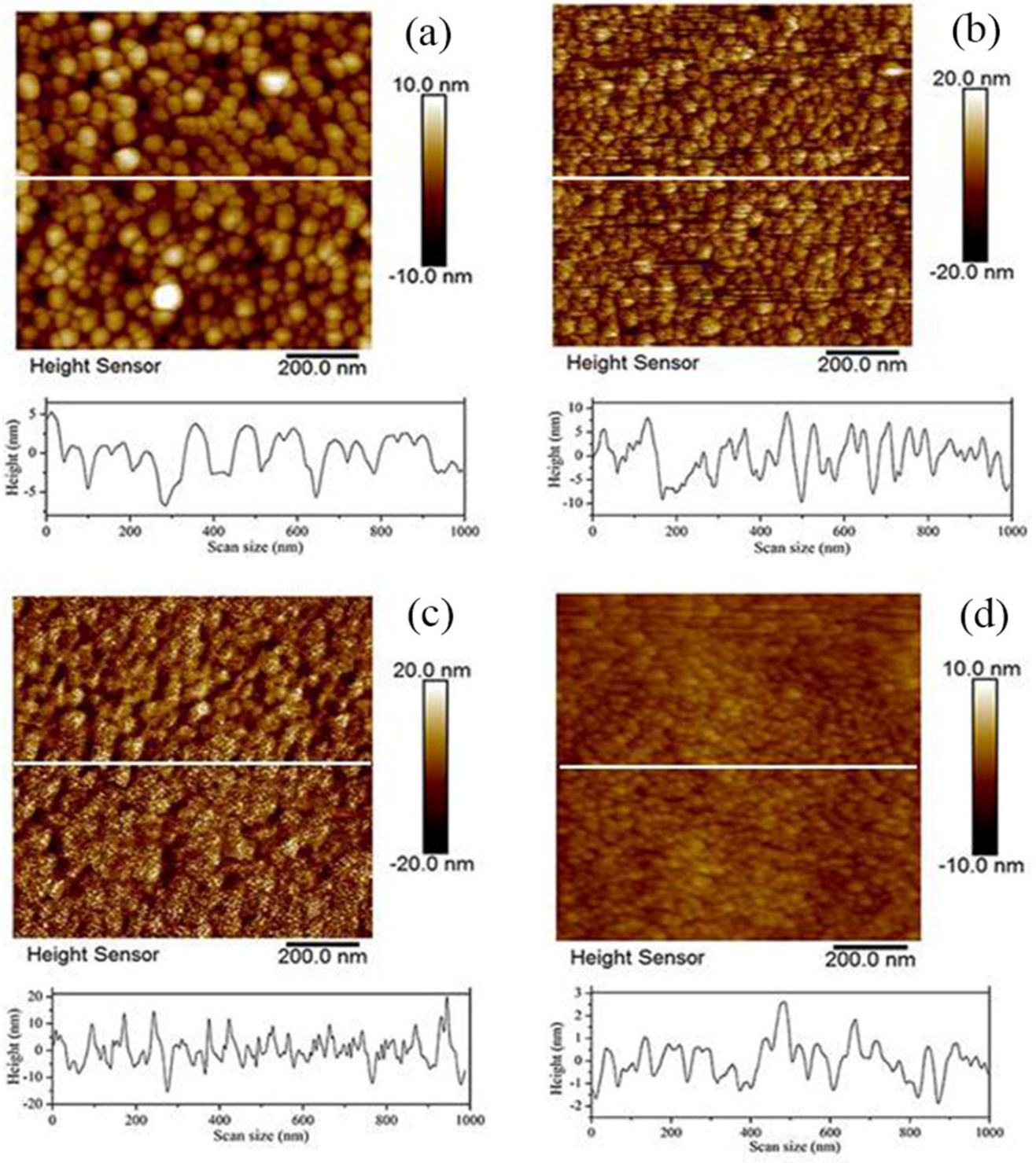

Figure 3: Two-dimensional (2D) AFM height images of Fe-doped ZnO thin films with different Fe contents: a) 0; b) 1%; c) 5%; d) 10%.

1.04:1 and 0.92:1, indicating that some Zn atomic lattice is replaced by Fe atom to form solid solution, which is consistent to the XRD analysis.

Figure 3a, Figure 3b, Figure 3c and Figure 3d show two-dimensional (2D) AFM surface height morphologies of xFe-ZnO thin films (x = 0, 1, 5 and 10 mol%). The scanning area is 1 μm^2. Each film was composed of many fine ZnO particles. Obviously, with the increasing Fe dopant content from 0, 1, 5 to 10 mol%, the average grain size of ZnO was decreased from 40, 30, 25 nm to 20 nm, which is conformed to the XRD results. Under each AFM image, the section of the white line in the image was

shown, indicating that the surface roughness was decreased after iron doping. However, in Figure 3d, excess Fe doping will increase the surface roughness due to the phase separation.

MFM is a kind of AFM, which scans magnetic samples with magnetic probes and detects the interaction between the probes and the samples to reconstruct the magnetic structure of the sample surface [14]. The samples were scanned by MFM with a scanning range of 1 μm^2. Antimony-doped silicon magnetic probe coated with cobalt-chromium alloy was used. The resonance frequency and the elastic modulus of the probe was 75 kHz and 2.8 N m^{-1}, respectively. When the magnetic disturbance between the tip and the sample is not considered, the formula for calculating the magnetic force of the sample can be obtained [15],

$$F = -\nabla E = \mu_0 \int \nabla \left(M_{tip} \cdot H_{sample} \right) dV_{tip} = \mu_0 \int \nabla \left(M_{sample} \cdot H_{tip} \right) dV_{sample} \quad (2)$$

That is, the convolution of the tip magnetic moment M_{tip} with the sample stray magnetic field H_{sample} or the convolution of the sample magnetic moment M_{sample} with the tip stray magnetic field H_{tip}. The corresponding MFM detection signal is proportional to the vertical component of the magnetic gradient, $\frac{\partial F}{\partial z}$. The vibration equation of the MFM probe is [16],

$$m\frac{d^2 z(t)}{dt^2} + my\frac{dz(t)}{dt} + \left(k_0 + \Delta k cos\left(\omega_m t \right) \right) z(t) = F_0 cos\left(\omega_c t \right) \quad (3)$$

Where z is the coordinate of the vibration direction of the probe, m is the effective mass of the probe, γ is the damping coefficient, k_0 is the spring constant, Δk is the variation of effective spring coefficient, ω_c is the driving frequency of piezoelectric elements, ω_m is the frequency of high frequency magnetic field, F_0 is the driving force of piezoelectric oscillator. The MFM probe can be considered as point magnetic charge q_{tip},

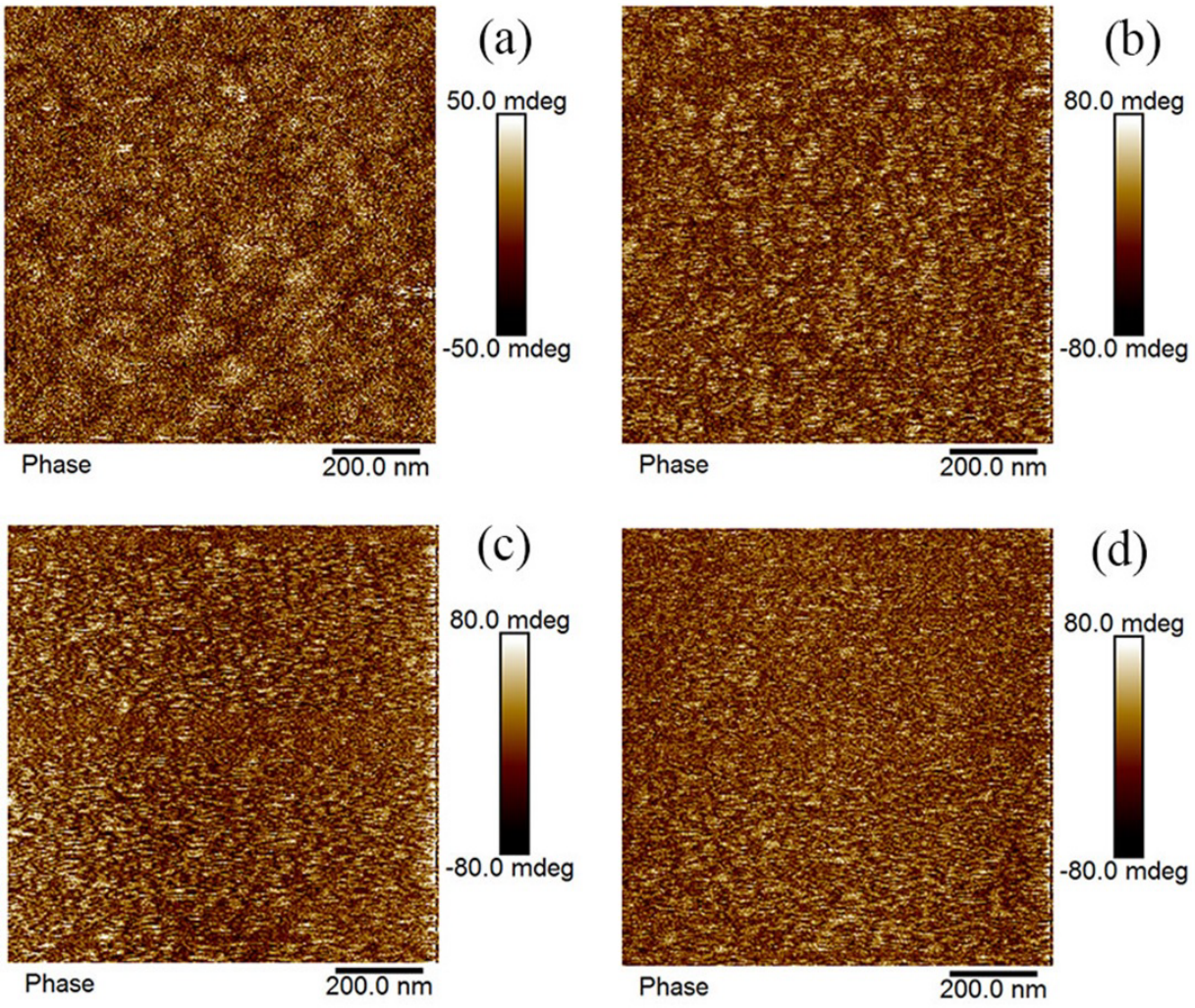

Figure 4: MFM height images of Fe-doped ZnO thin films with different Fe contents: a) 0; b) 1%; c) 5%; d) 10%.

consequently,

$$\Delta k = \frac{\partial F_m}{\partial z} = \frac{\partial}{\partial z} q_{tip} H_z cos(\omega_m t)$$

Where F_m is the alternating magnetic force between the probe and the sample, H_z is the amplitude of high frequency magnetic field. By adjusting the driving frequency of piezoelectric element ω_c to satisfy,

$$\omega_c - \omega_m = \omega_0 \quad (5)$$

Where ω_0 is the resonance frequency of the probe, as a result, the vibration signal of the probe is [17],

$$z(t) = \frac{F_0}{m\gamma\omega_0}\sin(\omega_c t) + \frac{F_0 \Delta k}{2(m\gamma\omega_0)^2} cos\left[(\omega_c - \omega_m)t\right] \quad (6)$$

Figure 4 is the MFM height images of ZnO thin films with different Fe content. Obviously, the intrinsic zinc oxide has no domain and magnetic moment distribution. After a certain amount of iron doping, the distribution of domain and magnetic moment is obtained. With the increase of iron doping, its magnetism tends to increase, the bright and dark fringes of domain are more clearly visible, indicating that a certain amount of iron doping can make the non-magnetic zinc oxide semiconductor become dilute magnetic semiconductor. However, when the iron doping content reaches 10%, its magnetic properties decrease, which indicates that iron doping has a most suitable proportion and is less than 10%.

Conclusions

In summary, a certain amount of iron doping can inhibit the growth of zinc oxide particles, and then grow more small crystal particles. With the increase of iron doping content, its magnetism tends to increase. A certain amount of iron doping can make non-magnetic zinc oxide semiconductor become dilute magnetic semiconductor, but the magnetism enhanced by iron doping is limited, and the upper limit is less than 10% of iron doping content. The surface roughness of the films increases with the increase of iron doping, because the stable solid solution cannot be formed due to the separation of two phases.

Acknowledgements

This work was financially supported by the Scientific and technological project of Henan province (182102210504), the national natural science foundation of China (51772256), the program for innovative research team (in science & technology) in university of Henan province (19IRTSTHN026).

References

1. RA Torquato, SE Shirsath, RHGA Kiminami, ACFM Costa (2018) Synthesis and structural, magnetic characterization of nanocrystalline $Zn_{1-x}Co_xO$ diluted magnetic semiconductors (DMS) synthesized by combustion reaction. Ceram Int 44: 4126-4131.
2. YD Zhang, LW Wang, LW Mi, FL Yang, Z Zheng (2011) Silica-controlled structure and optical properties of zinc oxide sol-gel thin films. J Mater Res 26: 882-888.
3. ZA Yunusov, SU Yuldashev, YH Kwon, DY Kim, SJ Lee, et al. (2018) Band gap engineering of ZnMnO diluted magnetic semiconductor by alloying with ZnS. J Mag Mag Mater 446: 206-209.
4. KY Salkar, RB Tangsali, RS Gad, U Subramanian (2019) Preparation characterization and magnetic properties of $Zn_{(1-x)}Co_xO$ nanoparticle Dilute magnetic semiconductors. Superlat Microstruct 126: 158-173.
5. C Belkhaoui, N Mzabi, H Smaoui (2019) Investigations on structural, optical and dielectric properties of Mn doped ZnO nanoparticles synthesized by co-precipitation method. Mater Res Bull 111: 70-79.
6. P Obreja, D Cristea, A Dinescu, C Romanitan (2019) Influence of surface substrates on the properties of ZnO nanowires synthesized by hydrothermal method. Appl Surf Sci 463: 1117-1123.
7. S Bose, D Sanyal (2018) Synthesis and characterization of ZnO microfiber by electrospinning technique. Mater Today: proceedings 5: 9860-9865.
8. R Nasser, H Elhouihet (2018) Production of acceptor complexes in sol-gel ZnO thin films by Sb doping. J Lumines 196: 11-19.
9. CBS Valentin, RLS Silva, P Banerjee, A Franco (2019) Investigation of Fe-doped room temperature dilute ma gnetic ZnO semiconductors. Mater Sci Semiconduct Proces 96: 122-126.
10. XF Jia, QY Hou, ZC Xu, LF Qu (2018) Effect of Ce doping on the magnetic and optical properties of ZnO by the first principle. J Mag & Mag Mater 465: 128-135.
11. KP Shinde, RC Pawar, BB Sinha, HS Kim, SS Oh, et al. (2014) Optical and magnetic properties of Ni doped ZnO planetary ball milled nanopowder synthesized by co-precipitation. Ceram Int 40: 16799-16804.
12. C Valentin, R Silva, P Banerjee, A Franco (2019) Investigation of Fe-doped room temperature dilute magnetic ZnO semiconductors. Mater Sci Semiconduct Processing 96: 122-126.

13.YD Zhang, HM Jia, PJ Li, FL Yang, Z Zheng (2011) Influence of glucose on the structural and optical properties of ZnO thin films prepared by sol-gel method. Opt Commun 284: 236-239.

14.MV Makarova, Y Akaishi, T Ikarshi, KS Rao, S Yoshimura, et al. (2019) Alternating Magnetic Force Microscopy: Effect of Si doping on the temporal performance degradation of amorphous FeCoB magnetic tips. J Mag & Mag Mater 471: 209-214.

15.I Utke, P Hoffmann, R Berger (2002) High-resolution magnetic Co supertips grown by a focused electron beam. Appl Phys Lett 80: 4792.

16.SL Tomlison, AN Farley (1997) The magnetic force microscopy and its capability for nanomagnetic studies. J Appl Phys 81: 5029.

17.SJL Vellekoop, L Abelmann, S Porthun, JC Lodder, JJ Miles (1999) Calculation of playback signals from MFM images using transfer functions. J Mag & Mag Mater 193: 474-478.

ISSN 2631-5084